



DIGITAL ACCESS TO SCHOLARSHIP AT HARVARD

Imaging of the unstable plaque: how far have we got?

The Harvard community has made this article openly available.
[Please share](#) how this access benefits you. Your story matters.

Citation	Matter, Christian M., Matthias Stuber, and Matthias Nahrendorf. 2009. Imaging of the unstable plaque: how far have we got?. European Heart Journal 30(21): 2566-2574.
Published Version	doi://10.1093/eurheartj/ehp419
Accessed	February 19, 2015 4:10:39 AM EST
Citable Link	http://nrs.harvard.edu/urn-3:HUL.InstRepos:4815536
Terms of Use	This article was downloaded from Harvard University's DASH repository, and is made available under the terms and conditions applicable to Other Posted Material, as set forth at http://nrs.harvard.edu/urn-3:HUL.InstRepos:dash.current.terms-of-use#LAA

(Article begins on next page)

Controversies in cardiovascular medicine series

Imaging of the unstable plaque: how far have we got?

Christian M. Matter^{1,2*}, Matthias Stuber^{3,4}, and Matthias Nahrendorf⁵

¹Cardiovascular Research, Institute of Physiology, Zurich Center for Integrative Human Physiology, University of Zurich, Zurich 8057, Switzerland; ²Cardiology, Cardiovascular Center, University Hospital Rämistrasse 100, 8091 Zürich, Switzerland; ³Division of Magnetic Resonance Research, Department of Radiology, Johns Hopkins University School of Medicine, Baltimore, MD 21287, USA; ⁴Department of Radiology, Centre Hospitalier Universitaire Vaudois and University of Lausanne, Lausanne 1011, Switzerland; and ⁵Center for Systems Biology, Massachusetts General Hospital and Harvard Medical School, Boston, MA 02114, USA

Received 30 June 2009; revised 31 August 2009; accepted 17 September 2009; online publish-ahead-of-print 15 October 2009

Rupture of unstable plaques may lead to myocardial infarction or stroke and is the leading cause of morbidity and mortality in western countries. Thus, there is a clear need for identifying these vulnerable plaques before the rupture occurs. Atherosclerotic plaques are a challenging imaging target as they are small and move rapidly, especially in the coronary tree. Many of the currently available imaging tools for clinical use still provide minimal information about the biological characteristics of plaques, because they are limited with respect to spatial and temporal resolution. Moreover, many of these imaging tools are invasive. The new generation of imaging modalities such as magnetic resonance imaging, nuclear imaging such as positron emission tomography and single photon emission computed tomography, computed tomography, fluorescence imaging, intravascular ultrasound, and optical coherence tomography offer opportunities to overcome some of these limitations. This review discusses the potential of these techniques for imaging the unstable plaque.

Keywords Atherosclerosis • Molecular imaging • Vulnerable plaque

Need for high resolution imaging of plaque biology

Acute coronary syndromes (ACS) are the most frequent cause of hospitalization in western countries and may be complicated by acute heart failure or sudden cardiac death. The underlying mechanism of ACS is plaque rupture, endothelial erosion, and/or intra-plaque haemorrhage with partial or complete occlusion of an epicardial coronary artery.

Mortality of the sequelae of ACS remains high. Instead of preventing ACS, we are frequently limited to diagnose evolving ACS by relying on electrocardiogram changes, chest pain, and markers of cardiomyocyte necrosis. In order to limit the damage, this leaves us with 'late' measures such as percutaneous interventions. Nevertheless, in the best case scenario, we fix the problem (thrombotic coronary artery occlusion) *after* the event (plaque rupture or erosion) occurred. Instead, prevention of this event with the identification of patients at risk for plaque rupture would be desirable.

Vulnerable plaques are characterized by increased inflammatory infiltrates (i.e. mainly monocytes/macrophages, some T-cells, and neutrophils). Upon ingestion of modified LDL, macrophages become foam cells and release inflammatory cytokines and proteases that induce fibrous cap thinning.^{1,2} Lipid-loaded foam cells eventually die, thereby leading to growth of the necrotic core.

Relying on inflammation as a central pathogenic aspect of plaque vulnerability, circulating inflammatory biomarkers of vulnerable plaques have been identified. They provide valuable diagnostic and prognostic information.³ However, they do not provide insight in the anatomic localization of vulnerable plaques. Thus, timely and anatomically precise imaging of vulnerable plaques is a medical need, since angiographic and pathological studies demonstrate that coronaries frequently occlude acutely without flow-limiting stenoses.^{4,5} These findings suggest that the biological characteristics of plaques rather than the degree of luminal narrowing determine the risk for coronary occlusion. X-ray coronary angiography only visualizes the coronary lumen and provides

* Corresponding author. Tel: +41 44 635 6467, Fax: +41 44 635 6827, Email: cmatter@physioluzh.ch

Published on behalf of the European Society of Cardiology. All rights reserved. © The Author 2009. For permissions please email: journals.permissions@oxfordjournals.org. The online version of this article has been published under an open access model. Users are entitled to use, reproduce, disseminate, or display the open access version of this article for non-commercial purposes provided that the original authorship is properly and fully attributed; the Journal, Learned Society and Oxford University Press are attributed as the original place of publication with correct citation details given; if an article is subsequently reproduced or disseminated not in its entirety but only in part or as a derivative work this must be clearly indicated. For commercial re-use, please contact journals.permissions@oxfordjournals.org.

minimal structural or biological information about the vessel wall. Thus, high resolution imaging of plaques reporting on critical lesion biology may identify patients at risk for ACS. Although a number of recent reviews have summarized novel imaging approaches aimed at achieving these goals,^{6–8} we here focus on novel imaging techniques that come close to fulfilling this promise in the near future (Table 1).

Targeted fluorescence imaging

Fluorescence imaging has revolutionized preclinical research because it is sensitive, cost-effective and can be used over a wide range from microscopic to macroscopic and *ex vivo* to *in vivo* applications. Currently, the main impact of optical imaging of inflamed atherosclerotic plaques is preclinical. Intravital microscopy⁹ and whole mouse tomographic imaging¹⁰ have targeted the key aspects of lesion biology. In addition, preclinical tools such as *ex vivo* immunofluorescence microscopy and flow cytometry are frequently used to validate novel imaging agents in rodent models. In particular, fluorescence molecular tomography holds promise for non-invasive imaging of murine models of atherosclerosis, because it allows quantification of tracer fluorochrome concentrations.¹¹ Comparable to positron emission tomography (PET)–computed tomography (CT), recent addition of hybrid anatomical imaging, for instance fluorescence-mediated tomography–CT, allows to exactly identify the anatomic source of molecular signals (Figure 1A).

Clinical translation of optical imaging has been hampered by physical hurdles, as light does not penetrate more than 8 cm of tissue. Although the use of fluorochromes in the near-infrared spectrum optimizes tissue penetration and minimizes autofluorescence,¹² the coronary artery tree is out of reach for non-invasive fluorescent sensing. However, carotid arteries should be accessible for non-invasive fluorescent imaging as they are closer to the body surface.

Recent advances in catheter-based technology allow to probe fluorescence in the vascular wall from inside the vessel (Figure 1B–E).¹³ For situations in which invasive angiography is needed, fluorescent sampling of the vascular wall may develop

into a valuable add-on as fluorescent probes can identify several hallmarks of lesion inflammation. Among these, activatable protease reporters are particularly promising.¹⁴ These probes are injected in a quenched, inactive state. Fluorochromes are attached to a polypeptide backbone, which is targeted by the protease of interest. Upon cleavage of the backbone by the enzyme, fluorochromes are liberated and gain a higher distance to each other, which renders them excitable with a laser in the appropriate wavelength.¹¹ After excitation, they emit light at a higher wavelength, detectable with appropriate charge-coupled device cameras or catheter sensors. In a hypothetical clinical scenario, pull-back scans of the coronary tree after systemic injection of an activatable fluorescent protease sensor may locate inflamed, vulnerable lesions in proximal coronary segments that have a high probability of causing ischaemic complications and therefore may warrant therapeutic intervention.

Nuclear imaging

The foremost advantage of nuclear imaging is its excellent sensitivity, which translates into the detection of sparse targets in the nanomolar range with low tracer doses. Until recently, single photon emission computed tomography (SPECT) and PET imaging of vascular biology were hampered by the low spatial resolution (4–10 mm) and limited ability to visualize anatomical detail. However, hybrid imaging of CT and magnetic resonance imaging (MRI) in dual modality systems exactly attribute the molecular signal to the anatomic source (Figure 2A–C). This progress has led to increased interest in the development of nuclear tracers for vascular applications.

¹⁸FDG (fluorodeoxyglucose) is a glucose analogon that enriches in metabolically active cells. It is clinically approved for cancer imaging and has been explored for imaging inflamed plaques with enhanced metabolism. Experimental and clinical studies suggest that ¹⁸FDG enriches in plaque macrophages and correlates with neovessel content.^{15–17} A limitation of ¹⁸FDG relates to its moderate specificity¹⁸ and the high background uptake in the myocardium, although some dietary measures may reduce cardiomyocyte uptake (Figure 2A and B).¹⁹ ¹⁸FDG is currently the only readily

Table 1 Tools for imaging the unstable plaque

Technique	Specificity	Sensitivity	Spatial Res	Temperature Res	Penetration	Clinical use	Specific features
Fluorescence I	++++	+++	++	+	+	(+)	Experimental
Nuclear I	++++	++++	+	+	++++	+++	Radiation
MRI	++	++	+++	+++	++++	++	No radiation
CT	+	+	+++	+++	++++	+++	Radiation
VH-IVUS	++	++	++	+++	++	+++	Invasive
OCT	++	+++	++++	++	+	++	Invasive, flushing
OFDI	++	+++	++++	++++	+	+	Invasive, no flushing
Angioscopy	+	+	+	+++	(+)	(+)	Invasive
Thermography	+	+	+	+	++	(+)	Invasive

MRI, magnetic resonance imaging; CT, computed tomography; VH-IVUS virtual histology-intravascular ultrasound; OCT, optical coherence tomography; OFDI, optical frequency domain imaging; temp, temporal; res, resolution.

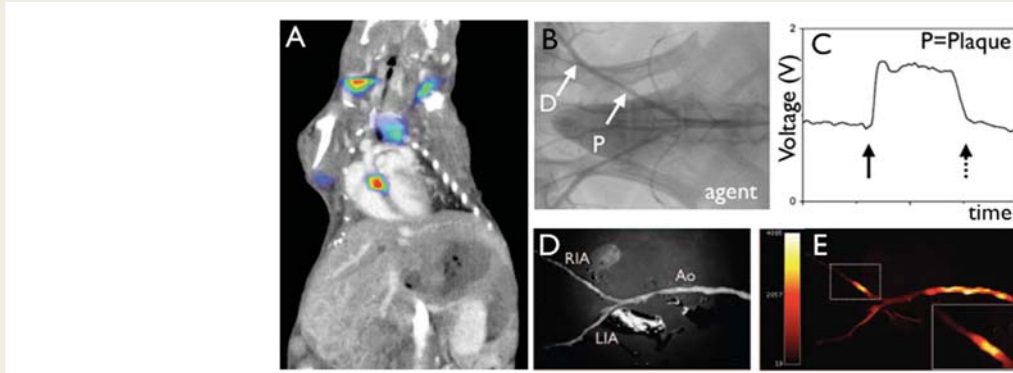


Figure 1 Fluorescence imaging of protease activity. (A) *In vivo* fluorescence molecular tomography (FMT) of an atherosclerotic mouse after injection of a cathepsin-targeted protease reporter. Hybrid FMT–CT imaging shows activation of the sensor in the aortic root, a site of strong inflammatory atherosclerosis in this model.⁷⁶ (B–E) Catheter-based sensing of fluorescence protease reporters in a rabbit model of arterial injury. The balloon injury was applied in the iliac artery (B). During pull back of a fluorescence sensing catheter, high signal was observed (C), corroborated by *ex vivo* fluorescence reflectance imaging (D, E).¹³

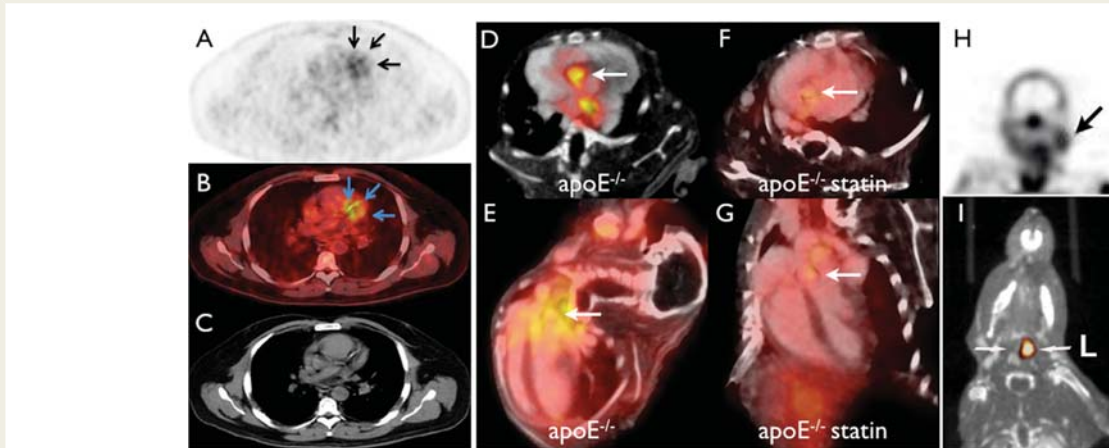


Figure 2 Nuclear imaging of plaque biology. (A–C) Clinical ¹⁸F-FDG PET–CT imaging in a patient with coronary artery disease shows uptake of the tracer in a stenotic segment (confirmed by angiography).¹⁹ (D–G) *In vivo* PET–CT imaging with the VCAM-1 targeted tracer ¹⁸F-4V in atherosclerotic mice with and without statin treatment. (D, F) Short-axis view of aortic root, (E and G) long-axis view. Statin therapy reduced VCAM-1 expression and consecutively PET signal. (H) SPECT imaging of apoptosis in the carotid artery of a TIA patient.²⁷ (I) *In vivo* MMP-targeted microSPECT–CT 3 weeks following carotid injury in the apoE^{−/−} mouse. Arrows point to the injured left (L) and non-injured right (R) carotid arteries.²⁸

available PET tracer for atherosclerotic studies and provides the possibility to explore PET–CT imaging for vascular targets in patients. Therefore, the number of clinical studies using ¹⁸F-FDG is on the rise.^{20,21}

Several tracers that target specific aspects of lesion biology are currently tested. Vascular cell adhesion molecule-1 (VCAM-1) is expressed early in the course of atherosclerotic disease, is favourably positioned on endothelial cells lining the inflamed plaque and therefore provides unhindered access for probes from the blood. Most importantly, VCAM-1 is central to both development and complications of atherosclerotic plaques. Monocytes/macrophages that are recruited into the subendothelial layer of the arterial wall bind to VCAM-1 via the integrin

VLA-4, a decisive step for cell extravasation. Vascular cell adhesion molecule-1 had been targeted with a variety of probes with magnetic, optical, and ultrasound reporters.^{22–24} More recently, a PET tracer has been developed²⁵, termed ¹⁸F-4V. Its good affinity, favourable pharmacokinetics and the choice of target make ¹⁸F-4V a promising candidate for translation (Figure 2D–G).

The trimodal nanoparticulate PET/MRI/optical agent ⁶⁴Cu-TNP was used to image a target downstream of VCAM-1, the presence of lesional macrophages.²⁶ The fluorescent properties of ⁶⁴Cu-TNP have been exploited to quantify the target cells by flow cytometric profiling of digested aortic plaques. Interestingly, this tracer is primarily taken up into macrophages. In a direct

comparison with high-field T2*-weighted MRI, the detection threshold was 50 times lower for PET detection.²⁶

Plaque foam cells eventually undergo apoptosis and form a necrotic core. Probes have been explored that target apoptosis using annexin-V as affinity ligand. Annexin-V binds to phosphatidylserine that is normally hidden on the inside of the cell membrane. In one small clinical study, increased uptake of ^{99m}Tc-labelled annexin-V in the carotid artery correlated with histological signs of apoptosis after endarterectomy.²⁷

Much of the mayhem caused by macrophages inside lesions is inflicted through protease activity. Released by monocytes/macrophages, these enzymes digest extracellular matrix and weaken the fibrous cap that protects the plaque against rupture. Several groups have developed small molecule inhibitors of matrix metalloproteinases and labelled these with radiotracers for SPECT imaging.^{28–30} Other matrix proteins such as the extradomain B of fibronectin³¹ and the C domain of tenascin-C³² are also increased in advanced plaques. Because these agents can visualize inflamed atherosclerotic plaques in mice, they may provide attractive opportunities for imaging advanced plaques in patients.

Macrophages deliver high payloads of vascular endothelial growth factor and may therefore stimulate growth of blood vessels. The leaky character of plaque neovessels has been inferred to promote intraplaque haemorrhage, further exacerbating inflammation.³³ Upon formation of these new microvessels, involved endothelial cells express a variety of integrins on their surface, which have been targeted using nuclear probes.³⁴ Frequently, affinity ligands binding to integrins incorporate the amino acid sequence Arg-Gly-Asp (RGD), which binds to $\alpha_v\beta_3$.³⁵ This integrin is also expressed by leucocytes, smooth muscle cells, and platelets. Some of these tracers have already been used in clinical studies.³⁶

Taken together, nuclear imaging techniques hold great promise for non-invasive detection of inflamed, rupture-prone atherosclerotic lesions. Their limited ability to provide anatomical detail has been overcome by hybrid CT or MRI. Although we are seeing the first PET images of coronary arteries in patients, the rapid motion and small size of these vascular territories still pose greater challenges than imaging of the carotid arteries.

Magnetic resonance imaging

Magnetic resonance imaging is a safe and non-invasive technique that operates without X-rays. Using MRI, contrast between different tissues can easily be obtained and amplified using contrast agents. These characteristics render MRI well positioned for monitoring atherosclerotic disease progression or to guide therapy. Since MRI is a relatively signal-insensitive technique when compared with CT or PET, long scanning times are required for improving spatial resolution.

The current gold standard for the identification of coronary artery stenoses is X-ray coronary angiography. However, it is invasive and associated with significant costs and radiation exposure. Magnetic resonance imaging has the potential to overcome some of these limitations. However, the technical challenges related to spatial resolution, contrast generation, and motion artefact suppression are significant. To date, results from the only multicenter trial³⁷ suggest that MRI can reliably identify significant proximal luminal

disease and rule out patients without significant proximal or three-vessel disease. However, the specificity of MRI is still relatively low. More advanced and promising approaches include whole heart coronary MR angiography³⁸ (Figure 3A–C), as well as the use of both high magnetic field strength³⁹ and molecular imaging agents.⁴⁰

On conventional coronary MRI, there is little contrast between the luminal blood and the coronary vessel wall. Using sophisticated magnetization preparation schemes,⁴¹ a high 'dark-blood' contrast between the coronary blood pool and the coronary vessel wall can be obtained.⁴² Building on this technique, positive coronary arterial remodelling was successfully quantified in patients with mild coronary artery disease.⁴³ Furthermore, this technique visualized differences in coronary vessel wall remodelling in high-risk diabetic patients with and without nephropathy (Figure 3D and E).⁴⁴

Magnetic resonance imaging was further refined for resolving plaque structure: multisequence MRI was able to detect unstable fibrous caps in advanced human carotid plaques.⁴⁵ In addition, after selecting patients with carotid artery stenosis via ultrasound, bilateral carotid MRI scans at 1.5 T identified complex lesions in a substantial number of arteries in the absence of high-grade narrowing.⁴⁶ Moreover, tools have been developed for MRI of coronary plaque components. Gadolinium (Gd) clearance is delayed in regions of carotid atherosclerotic plaques with thin fibrous caps ($<60\ \mu\text{m}$)⁴⁷ which was attributed to both inflammation and endothelial dysfunction. Later on, delayed signal enhancement in the coronary vessel wall after Gd identified patients with established coronary artery disease (Figure 3F).^{48,49} Similarly, enhanced contrast uptake was found in the coronary vessel wall of patients 6 days after AMI⁵⁰ and decreased 3 months later parallel to the declines in C-reactive protein. Thus, delayed Gd enhancement of the coronary vessel wall may be useful for visualization of inflammatory activity in patients with ACS. The question remains whether delayed Gd enhancement identifies plaques at risk for rupture. Of note, for some of these applications, the association between Gd exposure during MRI and the rare development of nephrogenic systemic fibrosis has to be considered when using Gd for plaque characterization.^{51,52}

A number of MRI-based strategies have been proposed for detecting inflammation in atherosclerotic plaques using targeted gadolinium agents⁵³ and superparamagnetic nanoparticles which are taken up by macrophages.⁵⁴ This notion was extended recently using a positive contrast off-resonance imaging sequence (inversion recovery with ON-resonant water suppression-MRI).⁵⁵ In combination with intravenously injected superparamagnetic nanoparticles (monocrystalline iron-oxide nanoparticles—MION-47), this technique generated positive contrast in areas of plaque macrophages⁵⁶ in an animal model. Currently, the development of contrast agents that 'highlight' specific plaque components for MRI seems promising. So far, molecular agents targeted to adhesion molecules,²³ or high-density lipoprotein,⁵⁷ matrix metalloproteinases,⁵⁸ and macrophage scavenger receptors⁵⁹ have been tested at the preclinical level, and agents targeted to fibrin⁶⁰ and macrophages⁶¹ have already been used in patients.

In summary, translation of molecular MRI to clinical applications appears particularly promising in combination with above-mentioned MRI techniques for coronary vessel wall imaging.

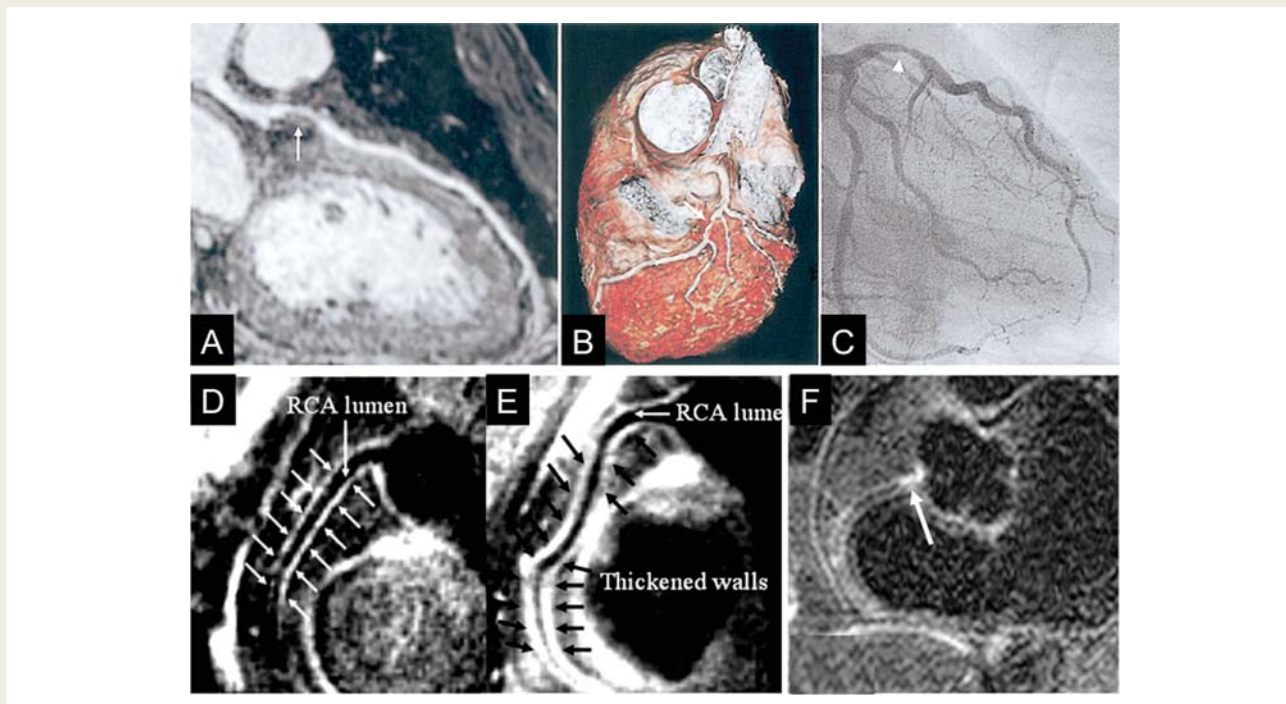


Figure 3 Visualization of a coronary atherosclerosis by MRI. (A) Curved multiplanar reconstruction of a whole-heart coronary MRA data acquisition shows a stenosis in the left anterior descending (LAD) artery (arrow). (B) Volume-rendering method in the same patient demonstrates three-dimensional view of the LAD with stenosis (white arrows). (C) X-ray coronary angiography confirms the stenosis of the proximal LAD (arrowhead),³⁸ reprinted with permission from Elsevier. (D and E) Coronary vessel wall images of the proximal RCA in two other subjects without coronary luminal stenoses; (D) a 58-year-old man with long-standing type 1 diabetes and normoalbuminuria and (E) a 44-year-old man with long-standing type 1 diabetes and diabetic nephropathy. In (D), there is no evidence of atherosclerotic plaque. However, an increased atherosclerotic plaque burden is seen in (E). The anterior and posterior RCA walls are indicated by arrows⁴⁴ reprinted with permission from Wolters Kluwer Health. (F) Delayed focal gadolinium late enhancement of the proximal RCA (arrow) is shown in another patient with X-ray defined coronary artery disease in the same location,⁴⁸ reprinted by permission of the European Society of Cardiology.

Computed tomography

Recent technological advances including multi-detector CT, dual-source CT, and ECG-gated CT led to a growing interest in CT as a tool for non-invasive characterization of coronary artery disease. When compared with MRI, CT is more signal-efficient and high-spatial resolution images of the entire coronary arterial tree can be obtained in a short period of sustained respiration, thereby markedly reducing scanning time. However, exposure to X-ray remains a concern and iodinated contrast agents are needed. Thus, imaging of low-risk subjects and repeated studies should not be performed.⁶² There has been a large number of recent single centre trials that examined the sensitivity and specificity of coronary CT angiography (CTA) in comparison to X-ray angiography. Consistent with the results from these studies, findings from a recent international multicenter trial⁶³ suggest that coronary 64-row multi-detector CTA is accurate in identifying coronary stenoses and characterizing disease severity in symptomatic patients who have coronary calcium scores of 600 or less. However, multi-detector CTA cannot currently be used as a substitute of conventional coronary angiography given its negative predictive value of 83% and positive predictive value of 91%.

With iodinated contrast agents, Hounsfield units can be measured directly and the expectation was that plaques or their components can be characterized based on X-ray attenuation. Due to considerable overlap in the attenuation spectrum of lipid and fibrous tissue,⁶⁴ most of the contemporary CT methods unfortunately cannot identify unstable plaques. However, an iodinated contrast agent with specificity for plaque macrophages recently improved visualization of plaque macrophages in an atherosclerotic rabbit model.⁶⁵

Intravascular ultrasound

Intravascular ultrasound (IVUS) is an invasive, catheter-based imaging technique that provides two-dimensional cross-sectional images of the whole arterial wall. The high accuracy of IVUS to measure lumen, plaque, and vessel area as well as morphological features is established. Given its axial resolution $\sim 100 \mu\text{m}$ using 40 MHz detectors, IVUS has the ability to localize plaques and quantify plaque burden. Moreover, IVUS is able to identify echolucent areas that represent lipid-rich plaques and may thus have the potential to identify unstable plaques by quantifying necrotic cores in coronary arteries.⁶⁶ However, given the limited specificity of

echolucency, the restricted access to proximal coronary segments, its moderate sensitivity to detect lipid-rich lesions and fibrous cap thickness, this technique has not yet reached clinical routine.

Advances in IVUS technology, i.e. spectral analysis of the IVUS backscatter radiofrequency signal have further improved the tissue characterization of plaques to a degree that it is referred to as virtual histology (VH-IVUS); the raw signals from reflection of ultrasound waves are transduced into a colour-coded representation of plaque characteristics.⁶⁷ During recent years, VH-IVUS has been extensively validated. *Ex vivo* analyses of human plaque specimens showed that VH-IVUS could identify plaque components such as lipids, fibrous tissue, calcifications, and the necrotic core.⁶⁸ Some limitations were reported in a porcine model of complex coronary lesions in which VH-IVUS was not accurate in detecting the relative amount of specific plaque components within each corresponding histological specimen.⁶⁹ In patients with ACS or stable coronary artery disease, VH-IVUS detected thin-cap fibroatheroma as a morphological plaque feature associated with high-risk ACS presentation.⁷⁰ On the basis of these findings, VH-IVUS emerges as a promising tool for further characterization of vulnerable plaques.

Optical coherence tomography

Optical coherence tomography (OCT) represents a new optical analogue of ultrasound imaging and has been introduced as an intravascular imaging modality with excellent spatial resolution (10–15 μm) that provides cross-sectional images of the coronary arteries. When compared with IVUS, OCT facilitates the identification of intimal hyperplasia, the internal and external elastic laminae as well as echolucent regions. Optical coherence tomography can also detect and quantify the key pathological features of vulnerable plaques such as a thin fibrous cap (<65 μm) and a large lipid pool.⁷¹ The safety and feasibility of using an intravascular

OCT image wire system has been demonstrated in ACS patients as well as in patients with acute myocardial infarction.⁷² Furthermore, OCT has been used successfully to assess culprit lesion morphology *in vivo*⁷³ and restenosis after stenting.⁷⁴

A very attractive upgrade of OCT has recently been introduced: Fourier-domain-OCT, also called optical frequency domain imaging (OFDI) works at much higher frame rates (>100 frames/s). This technique enables rapid, three-dimensional imaging of long coronary segments from 3 to 7 cm at pullback rates >20 mm/s after a brief, non-occlusive saline purge,⁷⁵ therefore eliminating the necessity to use a closure balloon.

Imaging the unstable plaque—present and future

How can aforementioned imaging modalities be used for imaging the unstable plaque?

Among the *anatomical* imaging tools (Figure 4, right), CT and MRI hold promise given their non-invasive character. Whereas MRI provides excellent soft tissue contrast and a better contrast resolution, CT allows much shorter scanning times. However, the hazard of exposing patients to radiation is a concern. The invasive approaches IVUS-VH and OCT/OFDI offer high-excellent spatial resolution. The combination of anatomical with *biological* imaging using hybrid techniques, i.e. PET–CT or PET–MRI, appears to be particularly attractive. Among those, targeted imaging that measures inflammation holds the greatest promise to identify unstable plaques by reporting on macrophages and other mechanisms involved in plaque vulnerability (Figure 4, left) such as adhesion molecules, proteases, and matrix components.

How should the patients be selected for plaque imaging and how should we manage these unstable plaques?

Optimal patient selection may be reached by integrating individual risk factors, clinical data, and key plasma biomarkers. Once

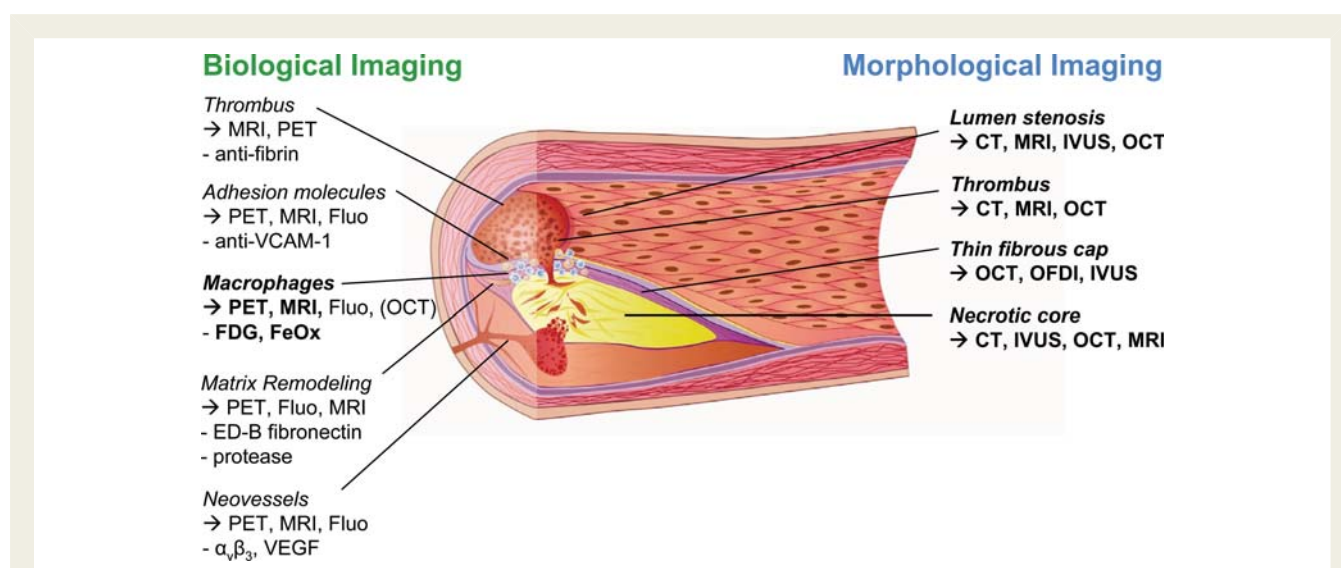


Figure 4 Techniques for imaging the unstable plaque. This scheme illustrates morphological and biological tools for visualizing vulnerable plaques. Modalities with clinical applications are given in bold.

critical lesions are identified, tailored interventions may reduce the risk of complications caused by the prospective culprit lesion. However, optimal management of unstable plaques remains to be defined and tested prospectively. Preventive or therapeutic options may include minimizing risk factors using life style changes, systemic drug therapy such as statins that reduce inflammation, and mechanical 'plaque sealing' using PCI. Currently, it is unclear if invasive 'cool down' of inflamed atherosclerotic lesions has a favourable risk–benefit ratio. Thus, the appropriate use of any plaque imaging modality and consecutive interventions need to be investigated in prospective clinical trials, ultimately leading to guidelines for identification, risk stratification, and therapy of patients with unstable plaques.

Funding

This work was supported by grants from the Swiss National Science Foundation 31-114094/1 (C.M.M.), the URPP 'Integrative Human Physiology' at the University of Zurich (C.M.M.), AHA SDG 0835623D (M.N.), and in part by the NIH grants R01HL095629-01 (M.N.), R01HL096576-01 (M.N.), R01-HL084186 (M.S.), R01-HL61912 (M.S.), and the Donald W. Reynolds Foundation (M.S.). Further support was provided by unrestricted grants from the MERCATOR Foundation Switzerland and a strategic alliance with Pfizer, Inc. New York. Funding to pay the Open Access publication charges for this article was provided by Cardiovascular Research Foundation Zurich.

Conflict of interest: none declared.

References

- Libby P. Inflammation in atherosclerosis. *Nature* 2002;**420**:868–874.
- Hansson GK. Inflammation, atherosclerosis, and coronary artery disease. *N Engl J Med* 2005;**352**:1685–1695.
- Zethelius B, Berglund L, Sundstrom J, Ingelsson E, Basu S, Larsson A, Venge P, Arnlov J. Use of multiple biomarkers to improve the prediction of death from cardiovascular causes. *N Engl J Med* 2008;**358**:2107–2116.
- Little WC, Constantinescu M, Applegate RJ, Kutcher MA, Burrows MT, Kahl FR, Santamore WP. Can coronary angiography predict the site of a subsequent myocardial infarction in patients with mild-to-moderate coronary artery disease? *Circulation* 1988;**78**:1157–1166.
- Falk E, Shah PK, Fuster V. Coronary plaque disruption. *Circulation* 1995;**92**:657–671.
- Fayad ZA. Cardiovascular molecular imaging. *Arterioscler Thromb Vasc Biol* 2009;**29**:981–982.
- Shaw SY. Molecular imaging in cardiovascular disease: targets and opportunities. *Nat Rev Cardiol* 2009;**6**:569–579.
- Nahrendorf M, Sosnovik D, French B, S FK, Bengel F, Sadeghi MM, Lindner JR, Wu JC, Kraitchman DL, Fayad ZA, Sinusas AJ. Multimodality cardiovascular molecular imaging, part II. *Circ Cardiovasc Imaging* 2009;**2**:56–70.
- Aikawa E, Aikawa M, Libby P, Figueiredo JL, Rusanescu G, Iwamoto Y, Fukuda D, Kohler RH, Shi GP, Jaffer FA, Weissleder R. Arterial and aortic valve calcification abolished by elastolytic cathepsin S deficiency in chronic renal disease. *Circulation* 2009;**119**:1785–1794.
- Chen J, Tung CH, Mahmood U, Ntziachristos V, Gyurko R, Fishman MC, Huang PL, Weissleder R. In vivo imaging of proteolytic activity in atherosclerosis. *Circulation* 2002;**105**:2766–2771.
- Ntziachristos V, Tung CH, Bremer C, Weissleder R. Fluorescence molecular tomography resolves protease activity in vivo. *Nat Med* 2002;**8**:757–760.
- Weissleder R, Ntziachristos V. Shedding light onto live molecular targets. *Nat Med* 2003;**9**:123–128.
- Jaffer FA, Vinegoni C, John MC, Aikawa E, Gold HK, Finn AV, Ntziachristos V, Libby P, Weissleder R. Real-time catheter molecular sensing of inflammation in proteolytically active atherosclerosis. *Circulation* 2008;**118**:1802–1809.
- Jaffer FA, Kim DE, Quinti L, Tung CH, Aikawa E, Pande AN, Kohler RH, Shi GP, Libby P, Weissleder R. Optical visualization of cathepsin K activity in atherosclerosis with a novel, protease-activatable fluorescence sensor. *Circulation* 2007;**115**:2292–2298.
- Aziz K, Berger K, Claycombe K, Huang R, Patel R, Abela GS. Noninvasive detection and localization of vulnerable plaque and arterial thrombosis with computed tomography angiography/positron emission tomography. *Circulation* 2008;**117**:2061–2070.
- Calcagno C, Cornily JC, Hyafil F, Rudd JH, Briley-Saebo KC, Mani V, Goldschlager G, Machac J, Fuster V, Fayad ZA. Detection of neovessels in atherosclerotic plaques of rabbits using dynamic contrast enhanced MRI and 18F-FDG PET. *Arterioscler Thromb Vasc Biol* 2008;**28**:1311–1317.
- Tawakol A, Migrino RQ, Bashian GG, Bedri S, Vermeylen D, Cury RC, Yates D, LaMuraglia GM, Furie K, Houser S, Gewirtz H, Muller JE, Brady TJ, Fischman AJ. In vivo 18F-fluorodeoxyglucose positron emission tomography imaging provides a noninvasive measure of carotid plaque inflammation in patients. *J Am Coll Cardiol* 2006;**48**:1818–1824.
- Matter CM, Wyss MT, Meier P, Spath N, von Lukowicz T, Lohmann C, Weber B, Ramirez de Molina A, Lacal JC, Ametamey SM, von Schulthess GK, Luscher TF, Kaufmann PA, Buck A. 18F-choline images murine atherosclerotic plaques ex vivo. *Arterioscler Thromb Vasc Biol* 2006;**26**:584–589.
- Wykrzykowska J, Lehman S, Williams G, Parker JA, Palmer MR, Varkey S, Kolodny G, Laham R. Imaging of inflamed and vulnerable plaque in coronary arteries with 18F-FDG PET/CT in patients with suppression of myocardial uptake using a low-carbohydrate, high-fat preparation. *J Nucl Med* 2009;**50**:563–568.
- Rudd JH, Myers KS, Bansilal S, Machac J, Pinto CA, Tong C, Rafique A, Hargeaves R, Farkouh M, Fuster V, Fayad ZA. Atherosclerosis inflammation imaging with 18F-FDG PET: carotid, iliac, and femoral uptake reproducibility, quantification methods, and recommendations. *J Nucl Med* 2008;**49**:871–878.
- Tahara N, Kai H, Ishibashi M, Nakaura H, Kaida H, Baba K, Hayabuchi N, Imaizumi T. Simvastatin attenuates plaque inflammation: evaluation by fluorodeoxyglucose positron emission tomography. *J Am Coll Cardiol* 2006;**48**:1825–1831.
- Behm CZ, Kaufmann BA, Carr C, Lankford M, Sanders JM, Rose CE, Kaul S, Lindner JR. Molecular imaging of endothelial vascular cell adhesion molecule-1 expression and inflammatory cell recruitment during vasculogenesis and ischemia-mediated arteriogenesis. *Circulation* 2008;**117**:2902–2911.
- Nahrendorf M, Jaffer FA, Kelly KA, Sosnovik DE, Aikawa E, Libby P, Weissleder R. Noninvasive vascular cell adhesion molecule-1 imaging identifies inflammatory activation of cells in atherosclerosis. *Circulation* 2006;**114**:1504–1511.
- McAtteer MA, Schneider JE, Ali ZA, Warrick N, Bursill CA, von zur Muhlen C, Greaves DR, Neubauer S, Channon KM, Choudhury RP. Magnetic resonance imaging of endothelial adhesion molecules in mouse atherosclerosis using dual-targeted microparticles of iron oxide. *Arterioscler Thromb Vasc Biol* 2008;**28**:77–83.
- Nahrendorf M, Keliher E, Panizzi P, Zhang H, Hembrador S, Figueiredo JL, Aikawa E, Kelly K, Libby P, Weissleder R. ¹⁸F-4V for PER-CT imaging of VCAM-1 expression in atherosclerosis. *JACC Cardiovasc Imaging* 2009;**2**:1213–1222.
- Nahrendorf M, Zhang H, Hembrador S, Panizzi P, Sosnovik DE, Aikawa E, Libby P, Swirski FK, Weissleder R. Nanoparticle PET–CT imaging of macrophages in inflammatory atherosclerosis. *Circulation* 2008;**117**:379–387.
- Kietselaer BL, Reutelingsperger CP, Heidendal GA, Daemen MJ, Mess WH, Hofstra L, Narula J. Noninvasive detection of plaque instability with use of radio-labeled annexin A5 in patients with carotid-artery atherosclerosis. *N Engl J Med* 2004;**350**:1472–1473.
- Zhang J, Nie L, Razavian M, Ahmed M, Dobrucki LW, Asadi A, Edwards DS, Azure M, Sinusas AJ, Sadeghi MM. Molecular imaging of activated matrix metalloproteinases in vascular remodeling. *Circulation* 2008;**118**:1953–1960.
- Su H, Spinale FG, Dobrucki LW, Song J, Hua J, Sweterlitsch S, Dione DP, Cavaliere P, Chow C, Bourke BN, Hu XY, Azure M, Yalamanchili P, Liu R, Cheesman EH, Robinson S, Edwards DS, Sinusas AJ. Noninvasive targeted imaging of matrix metalloproteinase activation in a murine model of postinfarction remodeling. *Circulation* 2005;**112**:3157–3167.
- Schafers M, Riemann B, Kopka K, Breyholz HJ, Wagner S, Schafers KP, Law MP, Schober O, Levkau B. Scintigraphic imaging of matrix metalloproteinase activity in the arterial wall in vivo. *Circulation* 2004;**109**:2554–2559.
- Matter CM, Schuler PK, Alessi P, Meier P, Ricci R, Zhang D, Halin C, Castellani P, Zardi L, Hofer CK, Montani M, Neri D, Luscher TF. Molecular imaging of atherosclerotic plaques using a human antibody against the extra-domain B of fibronectin. *Circ Res* 2004;**95**:1225–1233.
- von Lukowicz T, Silacci M, Wyss MT, Trachsel E, Lohmann C, Buck A, Luscher TF, Neri D, Matter CM. Human antibody against C domain of tenascin-C visualizes murine atherosclerotic plaques ex vivo. *J Nucl Med* 2007;**48**:582–587.
- Kolodgie FD, Gold HK, Burke AP, Fowler DR, Kruth HS, Weber DK, Farb A, Guerrero LJ, Hayase M, Kutys R, Narula J, Finn AV, Virmani R. Intraplaque hemorrhage and progression of coronary atheroma. *N Engl J Med* 2003;**349**:2316–2325.
- Sadeghi MM, Krassilnikova S, Zhang J, Gharai AA, Fassaei HR, Esmailzadeh L, Kooshkabad A, Edwards S, Yalamanchili P, Harris TD, Sinusas AJ, Zaret BL, Bender JR. Detection of injury-induced vascular remodeling by targeting activated α phavbeta3 integrin in vivo. *Circulation* 2004;**110**:84–90.

35. Hua J, Dobrucki LW, Sadeghi MM, Zhang J, Bourke BN, Cavaliere P, Song J, Chow C, Jahanshad N, van Royen N, Buschmann I, Madri JA, Mendizabal M, Sinusas AJ. Noninvasive imaging of angiogenesis with a ^{99m}Tc -labeled peptide targeted at $\alpha\text{v}\beta 3$ integrin after murine hindlimb ischemia. *Circulation* 2005;**111**:3255–3260.
36. Makowski MR, Ebersberger U, Nekolla S, Schwaiger M. *In vivo* molecular imaging of angiogenesis, targeting $\alpha\text{v}\beta 3$ integrin expression, in a patient after acute myocardial infarction. *Eur Heart J* 2008;**29**:2201.
37. Kim WY, Danias PG, Stuber M, Flamm SD, Plein S, Nagel E, Langerak SE, Weber OM, Pedersen EM, Schmidt M, Botnar RM, Manning WJ. Coronary magnetic resonance angiography for the detection of coronary stenoses. *N Engl J Med* 2001;**345**:1863–1869.
38. Sakuma H, Ichikawa Y, Chino S, Hirano T, Makino K, Takeda K. Detection of coronary artery stenosis with whole-heart coronary magnetic resonance angiography. *J Am Coll Cardiol* 2006;**48**:1946–1950.
39. Stuber M, Botnar RM, Fischer SE, Lamerichs R, Smink J, Harvey P, Manning WJ. Preliminary report on *in vivo* coronary MRA at 3 Tesla in humans. *Magn Reson Med* 2002;**48**:425–429.
40. Bi X, Carr J, Li D. Whole-heart coronary magnetic resonance angiography at 3 Tesla in 5 min with slow infusion of Gd-BOPTA, a high-relaxivity clinical contrast agent. *Magn Reson Med* 2007;**58**:1–7.
41. Edelman RR, Chien D, Kim D. Fast selective black blood MR imaging. *Radiology* 1991;**181**:655–660.
42. Fayad ZA, Fuster V, Fallon JT, Jayasundera T, Worthley SG, Helft G, Aguinaldo JG, Badimon JJ, Sharma SK. Noninvasive *in vivo* human coronary artery lumen and wall imaging using black-blood magnetic resonance imaging. *Circulation* 2000;**102**:506–510.
43. Kim WY, Stuber M, Bornert P, Kissinger KV, Manning WJ, Botnar RM. Three-dimensional black-blood cardiac magnetic resonance coronary vessel wall imaging detects positive arterial remodeling in patients with nonsignificant coronary artery disease. *Circulation* 2002;**106**:296–299.
44. Kim WY, Astrup AS, Stuber M, Tarnow L, Falk E, Botnar RM, Simonsen C, Pietraszek L, Hansen PR, Manning WJ, Andersen NT, Parving HH. Subclinical coronary and aortic atherosclerosis detected by magnetic resonance imaging in type 1 diabetes with and without diabetic nephropathy. *Circulation* 2007;**115**:228–235.
45. Mitsumori LM, Hatsukami TS, Ferguson MS, Kerwin WS, Cai J, Yuan C. *In vivo* accuracy of multisequence MR imaging for identifying unstable fibrous caps in advanced human carotid plaques. *J Magn Reson Imaging* 2003;**17**:410–420.
46. Saam T, Underhill HR, Chu B, Takaya N, Cai J, Polissar NL, Yuan C, Hatsukami TS. Prevalence of American Heart Association type VI carotid atherosclerotic lesions identified by magnetic resonance imaging for different levels of stenosis as measured by duplex ultrasound. *J Am Coll Cardiol* 2008;**51**:1014–1021.
47. Wasserman BA, Smith WI, Trout HH III, Cannon RO III, Balaban RS, Arai AE. Carotid artery atherosclerosis: *in vivo* morphologic characterization with gadolinium-enhanced double-oblique MR imaging initial results. *Radiology* 2002;**223**:566–573.
48. Maintz D, Ozgun M, Hoffmeier A, Fischbach R, Kim WY, Stuber M, Manning WJ, Heindel W, Botnar RM. Selective coronary artery plaque visualization and differentiation by contrast-enhanced inversion prepared MRI. *Eur Heart J* 2006;**27**:1732–1736.
49. Yeon SB, Sabir A, Clouse M, Martinezclark PO, Peters DC, Hauser TH, Gibson CM, Nezafat R, Maintz D, Manning WJ, Botnar RM. Delayed-enhancement cardiovascular magnetic resonance coronary artery wall imaging: comparison with multislice computed tomography and quantitative coronary angiography. *J Am Coll Cardiol* 2007;**50**:441–447.
50. Ibrahim T, Makowski MR, Jankauskas A, Maintz D, Karch M, Schachoff S, Manning WJ, Schomig A, Schwaiger M, Botnar RM. Serial contrast-enhanced cardiac magnetic resonance imaging demonstrates regression of hyperenhancement within the coronary artery wall in patients after acute myocardial infarction. *JACC Cardiovasc Imaging* 2009;**2**:580–588.
51. Cowper SE, Robin HS, Steinberg SM, Su LD, Gupta S, LeBoit PE. Scleromyxoedema-like cutaneous diseases in renal-dialysis patients. *Lancet* 2000;**356**:1000–1001.
52. Daram SR, Cortese CM, Bastani B. Nephrogenic fibrosing dermopathy/nephrogenic systemic fibrosis: report of a new case with literature review. *Am J Kidney Dis* 2005;**46**:754–759.
53. Botnar RM, Perez AS, Witte S, Wiethoff AJ, Laredo J, Hamilton J, Quist W, Parsons EC Jr, Vaidya A, Kolodziej A, Barrett JA, Graham PB, Weisskoff RM, Manning WJ, Johnstone MT. *In vivo* molecular imaging of acute and subacute thrombosis using a fibrin-binding magnetic resonance imaging contrast agent. *Circulation* 2004;**109**:2023–2029.
54. Ruehm SG, Corot C, Vogt P, Kolb S, Debatin JF. Magnetic resonance imaging of atherosclerotic plaque with ultrasmall superparamagnetic particles of iron oxide in hyperlipidemic rabbits. *Circulation* 2001;**103**:415–422.
55. Stuber M, Gilson WD, Schar M, Kedziorek DA, Hofmann LV, Shah S, Vonken EJ, Bulte JW, Kraitman DL. Positive contrast visualization of iron oxide-labeled stem cells using inversion-recovery with ON-resonant water suppression (IRON). *Magn Reson Med* 2007;**58**:1072–1077.
56. Korosoglou G, Tang L, Kedziorek D, Cosby K, Gilson WD, Vonken EJ, Schar M, Sosnovik D, Kraitman DL, Weiss RG, Weissleder R, Stuber M. Positive contrast MR-lymphography using inversion recovery with ON-resonant water suppression (IRON). *J Magn Reson Imaging* 2008;**27**:1175–1180.
57. Frias JC, Williams KJ, Fisher EA, Fayad ZA. Recombinant HDL-like nanoparticles: a specific contrast agent for MRI of atherosclerotic plaques. *J Am Chem Soc* 2004;**126**:16316–16317.
58. Amirbekian V, Aguinaldo JG, Amirbekian S, Hyafil F, Vucic E, Sirol M, Weinreb DB, Le Gneur S, Lancelot E, Corot C, Fisher EA, Galis ZS, Fayad ZA. Atherosclerosis and matrix metalloproteinases: experimental molecular MR imaging *in vivo*. *Radiology* 2009;**251**:429–438.
59. Lipinski MJ, Frias JC, Amirbekian V, Briley-Saebo KC, Mani V, Samber D, Abbate A, Aguinaldo JG, Massey D, Fuster V, Vetrovec GW, Fayad ZA. Macrophage-specific lipid-based nanoparticles improve cardiac magnetic resonance detection and characterization of human atherosclerosis. *JACC Cardiovasc Imaging* 2009;**2**:637–647.
60. Spuentrup E, Botnar RM, Wiethoff AJ, Ibrahim T, Kelle S, Katoh M, Ozgun M, Nagel E, Vymazal J, Graham PB, Gunther RW, Maintz D. MR imaging of thrombi using EP-2104R, a fibrin-specific contrast agent: initial results in patients. *Eur Radiol* 2008;**18**:1995–2005.
61. Kooi ME, Cappendijk VC, Cleutjens KB, Kessels AG, Kitslaar PJ, Borgers M, Frederik PM, Daemen MJ, van Engelsehoven JM. Accumulation of ultrasmall superparamagnetic particles of iron oxide in human atherosclerotic plaques can be detected by *in vivo* magnetic resonance imaging. *Circulation* 2003;**107**:2453–2458.
62. Budoff MJ, Achenbach S, Blumenthal RS, Carr JJ, Goldin JG, Greenland P, Guerci AD, Lima JA, Rader DJ, Rubin GD, Shaw LJ, Wiegers SE. Assessment of coronary artery disease by cardiac computed tomography: a scientific statement from the American Heart Association Committee on Cardiovascular Imaging and Intervention, Council on Cardiovascular Radiology and Intervention, and Committee on Cardiac Imaging, Council on Clinical Cardiology. *Circulation* 2006;**114**:1761–1791.
63. Miller JM, Rochitte CE, Dewey M, Arbab-Zadeh A, Niinuma H, Gottlieb I, Paul N, Clouse ME, Shapiro EP, Hoe J, Lardo AC, Bush DE, de Roos A, Cox C, Brinker J, Lima JA. Diagnostic performance of coronary angiography by 64-row CT. *N Engl J Med* 2008;**359**:2324–2336.
64. Hoffmann U, Moselewski F, Nieman K, Jang IK, Ferencik M, Rahman AM, Cury RC, Abbata S, Joneidi-Jafari H, Achenbach S, Brady TJ. Noninvasive assessment of plaque morphology and composition in culprit and stable lesions in acute coronary syndrome and stable lesions in stable angina by multidetector computed tomography. *J Am Coll Cardiol* 2006;**47**:1655–1662.
65. Hyafil F, Cornily JC, Feig JE, Gordon R, Vucic E, Amirbekian V, Fisher EA, Fuster V, Feldman LJ, Fayad ZA. Noninvasive detection of macrophages using a nanoparticulate contrast agent for computed tomography. *Nat Med* 2007;**13**:636–641.
66. Ehara S, Kobayashi Y, Yoshiyama M, Shimada K, Shimada Y, Fukuda D, Nakamura Y, Yamashita H, Yamagishi H, Takeuchi K, Naruko T, Haze K, Becker AE, Yoshikawa J, Ueda M. Spotty calcification typifies the culprit plaque in patients with acute myocardial infarction: an intravascular ultrasound study. *Circulation* 2004;**110**:3424–3429.
67. Nair A, Kuban BD, Obuchowski N, Vince DG. Assessing spectral algorithms to predict atherosclerotic plaque composition with normalized and raw intravascular ultrasound data. *Ultrasound Med Biol* 2001;**27**:1319–1331.
68. Nair A, Kuban BD, Tuzcu EM, Schoenhagen P, Nissen SE, Vince DG. Coronary plaque classification with intravascular ultrasound radiofrequency data analysis. *Circulation* 2002;**106**:2200–2206.
69. Granada JF, Wallace-Bradley D, Win HK, Alviar CL, Builes A, Lev EI, Barrios R, Schulz DG, Raizner AE, Kaluza GL. *In vivo* plaque characterization using intravascular ultrasound-virtual histology in a porcine model of complex coronary lesions. *Arterioscler Thromb Vasc Biol* 2007;**27**:387–393.
70. Hong MK, Mintz GS, Lee CW, Lee JW, Park JH, Park DW, Lee SW, Kim YH, Cheong SS, Kim JJ, Park SW, Park SJ. A three-vessel virtual histology intravascular ultrasound analysis of frequency and distribution of thin-cap fibroatheromas in patients with acute coronary syndrome or stable angina pectoris. *Am J Cardiol* 2008;**101**:568–572.
71. Davies MJ. A macro and micro view of coronary vascular insult in ischemic heart disease. *Circulation* 1990;**82** (3 Suppl.):II38–II46.
72. Kubo T, Imanishi T, Takarada S, Kuroi A, Ueno S, Yamano T, Tanimoto T, Matsuo Y, Masho T, Kitabata H, Tsuda K, Tomobuchi Y, Akasaka T. Assessment of culprit lesion morphology in acute myocardial infarction: ability of optical

- coherence tomography compared with intravascular ultrasound and coronary angiography. *J Am Coll Cardiol* 2007;**50**:933–939.
73. Jang IK, Tearney GJ, MacNeill B, Takano M, Moselewski F, Iftima N, Shishkov M, Houser S, Aretz HT, Halpern EF, Bouma BE. *In vivo* characterization of coronary atherosclerotic plaque by use of optical coherence tomography. *Circulation* 2005;**111**:1551–1555.
 74. Serruys PW, Ormiston JA, Onuma Y, Regar E, Gonzalo N, Garcia-Garcia HM, Nieman K, Bruining N, Dorange C, Miquel-Hebert K, Veldhof S, Webster M, Thuesen L, Dudek D. A bioabsorbable everolimus-eluting coronary stent system (ABSORB): 2-year outcomes and results from multiple imaging methods. *Lancet* 2009;**373**:897–910.
 75. Tearney GJ, Waxman S, Shishkov M, Vakoc BJ, Suter MJ, Freilich MI, Desjardins AE, Oh WY, Bartlett LA, Rosenberg M, Bouma BE. Three-dimensional coronary artery microscopy by intracoronary optical frequency domain imaging. *JACC Cardiovasc Imaging* 2008;**1**:752–761.
 76. Nahrendorf M, Waterman P, Thurber G, Groves K, Rajopadhye M, Panizzi P, Marinelli B, Aikawa E, Pittet MJ, Swirski FK, Weissleder R. Hybrid *in vivo* FMT-CT imaging of protease activity in atherosclerosis with customized nanosensors. *Arterioscler Thromb Vasc Biol* 2009;**29**:1444–1451.

CARDIOVASCULAR FLASHLIGHT

doi:10.1093/eurheartj/ehp335

Online publish-ahead-of-print 18 August 2009

Tuberculous pericarditis with constrictive physiology

Morten Kraen*, Markus Muller, and Per Björkman

Department of Cardiology, University of Lund Sweden, Sdr. Forstadsgatan, Malmö 20502, Skane, Sweden

* Corresponding author. Tel: +46 40 333997, Fax: +46 40 336209, Email: morten.kraen@skane.se

A previously healthy 28-year-old man presented with 1 week's history of chest pain, low-grade fever, and progressive dyspnoea. Minimal electrocardiographic changes were found; however, cardiac ultrasound revealed moderate amounts of pericardial fluid, inferolateral hypokinesia, and a left ventricular ejection fraction of 40% (Panel 1, arrow points to pericardial effusion). Computed tomographic thorax showed mediastinal lymphadenopathy and discrete left upper lobe infiltrates (Panel 2, arrow points to left upper lobe infiltrates). Pericardial drainage was performed, with initial negative diagnostic results.

Tuberculin skin test and an interferon- γ release assay for tuberculosis were both positive, and therapy for presumptive tuberculous pericarditis was initiated, including prednisolone. The diagnosis was later confirmed by positive cultures for *Mycobacterium tuberculosis* from sputum and pericardial fluid. Further testing showed resistance to several first-line tuberculosis drugs.

At this time, the patient had developed signs of increased central venous pressure and tachycardia without recurrent pericardial effusion. Cardiac magnetic resonance imaging showed signs of constriction with a diastolic septal shift (Panel 3, arrow points to diastolic shift of the septum). The visceral and parietal layers of the pericardium were markedly thickened (measuring 5–10 mm) and showed late gadolinium enhancement (Panels 4 and 5, arrow points to the visceral and parietal layers of the pericardium).

Antituberculous therapy was modified, and the dose of steroids has been gradually tapered. Hitherto, the patient's cardiac condition has been stable without overt signs of heart failure and with increased exercise capacity, so pericardial surgery has been postponed.

Multidrug-resistant tuberculosis with constrictive pericarditis is exceedingly rare. A multidisciplinary imaging approach was helpful in determining the extent of cardiac involvement and will be used to assess the therapeutic outcome of this potentially reversible condition.

